Applied Surface Science 283 (2013) 58–64

Contents lists available at SciVerse ScienceDirect

Applied Surface Science

journal homepage: www.elsevier.com/locate/apsusc

Preparation and LPG-gas sensing characteristics of p-type semiconducting $LaNbO_4$ ceramic material

C. Balamurugan [a], D.-W. Lee [a,*], A. Subramania [b]

[a] MEMS and Nanotechnology Laboratory, School of Mechanical Systems Engineering, Chonnam National University, Gwangju 500757, South Korea
[b] Centre for Nanoscience and Technology, Pondicherry University, Puducherry 605014, India

ARTICLE INFO

Article history:
Received 20 March 2013
Received in revised form 22 May 2013
Accepted 2 June 2013
Available online 13 June 2013

Keywords:
$LaNbO_4$
Nanopowder
LPG sensor
p-type semiconducting gas sensor.

ABSTRACT

Lanthanam niobate ($LaNbO_4$) nanopowder was synthesized by a low temperature solution-based process. Thermal analysis TG/DTA, XRD, SEM, TEM, EDX, impedance analysis and Brunauer-Emmett-Teller (BET) were used to characterize the precursor and the calcined $LaNbO_4$ powders. The gas sensing behavior of $LaNbO_4$ nanopowder was studied with gases like liquid petroleum gas (LPG), ammonia (NH_3), and ethanol (C_2H_5OH), as a function of various controlling factors like operating temperature, concentration of the gas and response time. It revealed that $LaNbO_4$ is a very promising material for the detection of LPG (80%) and NH_3 (59%) at relatively lower operating temperatures.

1. Introduction

The research for newer materials which can be employed for high performance solid-state gas sensors has resulted in the development of various oxide materials. Semi-conducting metal oxide materials like ZnO, TiO_2, SnO_2, In_2O_3, etc., have been exploited in the past because of their simplicity, low cost and possible real time measurement. Among various metal oxides, $LaNbO_4$ is an excellent ceramic oxide having high thermal and mechanical stability. It exhibits polymorphism viz. monoclinic and tetragonal phases [1]. $LaNbO_4$ is used in solid oxide fuel cells, hydrogen sensors, etc., because of its enhanced physical and chemical properties [2–4]. In the field of gas-sensing materials, $LaNbO_4$ could be considered as potential candidate for future developments of sensing materials. The gas sensing mechanism involves a redox reaction at the surface, leading to a change in the depletion layer of the grains which in turn changes the electrical resistance. The most common reaction that leads to change in conductance is the adsorption of gases on the material surface. Adsorption being a surface effect, surface area plays an important role in the sensing mechanism. In nanosized materials large fraction of atoms are present at the surface and these atoms are widely used to enhance the gas-sensing properties of semiconducting oxides. Hence, for the application of gas sensors, nanosized particles are desirable. Earlier work pertaining to the preparation of $LaNbO_4$ powder relied on methods such as solid state, spray pyrolysis and sol–gel process were used to prepare [5,6]. Several shortcomings are encountered during these processes due to heat treatments involved which results in higher temperatures that leads to high energy consumption. Also, limitations such as difficulty in controlling the component homogeneity, crystal size, stoichiometric ratio, and formation of undesirable phase, all of which to a great extent result in decrease of gas sensitivity for a given material. To eliminate the difficulties in getting homogeneous nanocrystalline stoichiometric compound, a new method of synthesis was tried. Due to the increased awareness of potential hazards in both industrial and domestic environments, there is a growing need to detect and monitor gases particularly those that are toxic and potentially explosive. LPG that is widely used as a common fuel for industrial and domestic purposes is potentially hazardous because of its explosive nature on account of leakage. NH_3 is harmful and toxic in nature, is utilized extensively in many chemical industries, refrigeration systems, fire power plants, etc. Therefore, it is necessary to develop good sensors for the detection of LPG and NH_3. Past two decades, considerable efforts have been devoted to fabricate various semiconducting gas-sensing materials because they can detect toxic gases, which are relevant for chemical industries, environmental protection, public safety, and human health.

In particular, high-temperature gas sensors are based on semiconducting metal oxides as they are economical, small in size, easy to handle, and have fast response to changes in gas concentration. They also have additional advantages in terms of long operating life, high reliability leading to a low failure rate and effectiveness in a harsh environment.

* Corresponding author. Tel.: +82 062 530 1684.
E-mail address: mems@jun.ac.kr (D.-W. Lee).

0169-4332/$ – see front matter © 2013 Published by Elsevier B.V.
http://dx.doi.org/10.1016/j.apsusc.2013.06.013

In this paper, we report for first time the LPG, NH_3 and ethanol sensing properties of nanocrystalline $LaNbO_4$ prepared by the solution-based method. The characteristics of $LaNbO_4$-based sensor have been studied by measuring resistance of the sensor material in air and then in a reducing gas environment. It has been observed that there is an increase in gas response when exposed to reducing gases like liquid petroleum gas (LPG) ammonia (NH_3) and ethanol (C_2H_5OH) at 250 °C. $LaNbO_4$-based sensor has very promising future for LPG detection in the low ppm range with a response time in the seconds range.

2. Experimental details

Niobium pentoxide, lathanam nitrate, citric acid, ammonium hydroxide, ammonium oxalate, hydrofluoric acid and hydrogen peroxide were purchased from Merck and CDH. All the chemicals were of reagent grade and used without further purification. Among the various niobium compound (niobium alkoxides and $NbCl_5$), niobium pentoxide was selected as a starting material of niobium source because it is not only inexpensive but also easy to control moisture susceptibility.

$LaNbO_4$ nanoparticles were synthesized by simple two step solution-based method. The first step is the preparation of hydrated Nb_2O_5 from Nb_2O_5. In which Nb_2O_5 was dissolved in hydrofluoric acid with a constant stirring for about 6 h at 60 °C temperature, Nb_2O_5 was dissolved in HF to form $[NbOF_5]^{2-}$ or $[NbF_7]^{2-}$ complex. To this, a freshly prepared aqueous solution of ammonium oxalate was added in excess, with rapid stirring to the solution heated at 65 °C. The required amount of the aqueous ammonia was then added drop-by-drop, after terminating the reaction, to get hydrous niobium oxide ($Nb_2O_5{\cdot}nH_2O$) as precipitate. This hydrous oxide was filtered and washed with 10% aqueous ammonia solution by centrifugation to eliminate fluoride free hydrated Nb_2O_5. The addition of ammonium oxalate helped to truncate the polynuclear chain associated with hydrous niobium ions during the neutralization process [7]. The prepared hydrous niobium oxide was then assayed at 1000 °C for 3 h to estimate the amount of niobium oxide (Nb_2O_5) present in the hydrous oxide.

The second step involved the dissolution of stoichiometric amount of hydrous niobium pentoxide and lanthanum nitrate in citric acid solution (2 mol/mol of metal ion) in the presence of H_2O_2. The mixture was stirred on a hot plate with a magnetic stirrer until the reactants were dissolved fully. We utilize in the midst of citric acid $C(OH)(COOH)(CH_2{\cdot}COOH)_2{\cdot}H_2O$ in this work. Citric acid has three carboxylic and one hydroxyl group for coordinating metal ions which helps in homogenous mixing to get the transparent yellow color solution. The pH of solution was maintained at around 7 by adding aqueous ammonia to it. Ammonia addition led to rapid evolution of O_2 and NH_3, and the solution turned colorless. Viscous gel was formed by dehydrating the solution on a hot plate at 200 °C. Further heating led to charring of the gel and formation of black precursor powder. This dried mass was calcined at 900 °C for 2 h, to get a novel $LaNbO_4$ nanopowder. The resultant powder was characterized and evaluated for gas sensor applications.

The as-prepared precursor powder was subjected to simultaneous differential thermal analysis (DTA) and thermogravimetric analysis (TGA) (Model: Pyris Diamond) at a heating rate of 10 °C/min from 30 to 900 °C to determine the phase formation and complete crystallization temperature of the precursor sample. X-ray diffraction measurements of the calcined $LaNbO_4$ powders were carried out using X-ray diffraction analyzer with Cu Kα radiation at room temperature. XRD data were obtained at $2\theta = 20–80°$, with a step size of 0.02° and a count time of 4 s. Scherer's equation was used to calculate the average crystallite size of the powder. The morphology of the samples was investigated by scanning electron microscopy (Model: Hitachi, SN-3400N). The particle size and compositional analyses were carried out using transmission electron microscopy (Model: Philips CM-200), and energy dispersive spectroscopy attached with TEM. For TEM investigation, Sample was prepared by deposition and evaporation of an ethanolic $LaNbO_4$ dispersion on a lacey-film Cu grid. Brunauer–Emmett–Teller (BET) analysis of prepared powder sample was carried out with a (Micrometrisics, ASAP 2020), applying N2 as adsorbate. Impedance measurement of the powder was carried out in the temperature range 30–175 °C in air environment. A Potentiostat/Galvanostat (Model: Micro auto lab type III) analyzer was used for the impedance measurement in the frequency range of 1 Hz–500 kHz.

For sensor studies, $LaNbO_4$ nanopowder was mixed with 2% poly-vinyl alcohol as a binder to form a paste which was coated onto a ceramic tube substrate provided with platinum wire electrodes for electrical contacts. The tube was about 8 mm in length, 2 mm in external diameter and 1.6 mm in internal diameter. The sensor element was then heat-treated at 500 °C for an hour to remove the residual polymer, which helped to make it rigid and impart its porous nature. A small nichrome alloy coil was placed inside the tube as a micro heater to provide the required operating temperatures. Chromel-alumel thermocouple (TC) was used to sense the temperature of the sensor. The schematic of sensor element used for the gas sensitivity studies is shown in Fig. 1. The gas sensing performance of the sensor was studied in a sealed test chamber (300 cm^3) made up of aluminum with a gas inlet and an outlet. The test gases were injected into the test chamber through an injection part and the resistance was measured as a function of time until steady values were attained. The chamber was then purged with fresh air and the experiments were repeated. The electric circuit for the gas response measurement is shown in Fig. 2. The operating voltage (V_h) was supplied to either of the coils for heating the sensors and the circuit voltage ($V_C = 10$ V) was supplied across the sensors and the load resistor ($R_L = 1$ MΩ) connected in series. The signal voltage across the load, which changed with minute concentration of gas, was measured. For the p-type semiconducting material following formula is used for sensor response (S) calculation [8].

$$S(\%) = \frac{(R_g - R_a)}{R_a} \times 100 \quad (1)$$

R_g is the resistance under a given gas concentration at constant temperature and, R_a is the base resistance at constant temperature under gas-free atmosphere (dry air). In this study, the gas sensing properties of $LaNbO_4$ was investigated for LPG, NH_3 and ethanol from 50 to 350 °C. At the optimal operating temperature, the sensor

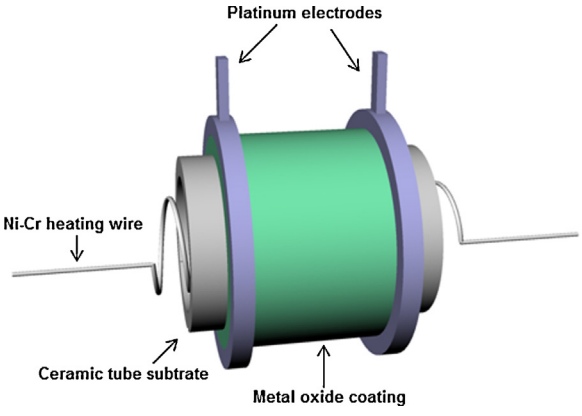

Fig. 1. The schematic of sensor element used for the gas response studies.

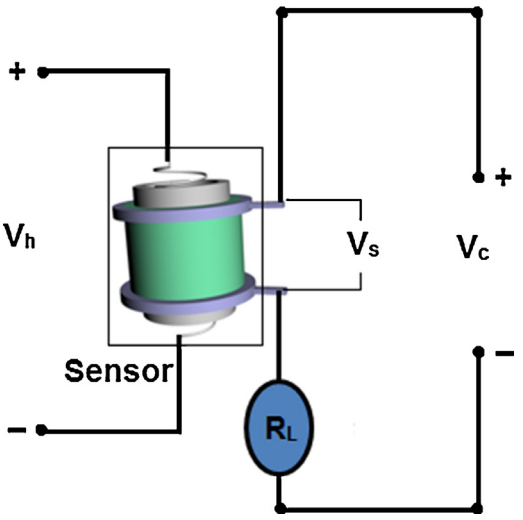

Fig. 2. Electrical circuit of the gas response test system (V_h: heating voltage, V_c: circuit voltage, V_c: output signal voltage and RL: load resistance).

response was measured as a function of various concentrations of test gases as well as response time.

3. Results and discussion

The thermal decomposition of $LaNbO_4$ precursor was evaluated at temperatures ranging from 30 to 900 °C using TG/DTA analysis as shown in Fig. 3. The endothermic peak on the DTA curves centered at 128 °C, together with drastic weight loss in the TG curve (19%), which corresponds to the evaporation of residual water and chemically bound water in the precursor sample. The first exothermic peak occurred with a huge mass loss of 30% and centered at 363 °C, representing the reaction of nitrates with citric acid and decomposition of the residual organic matter with the liberation of CO_2 and N_2. The generation of an enormous amount of heat facilitated formation of $LaNbO_4$. The last sharp exothermic peak occurred at 738 °C with mass loss. This is due to the phase transition of tetragonal $LaNbO_4$ to monoclinic phase or the co-existence of this phase together and crystallization of $LaNbO_4$. No more weight loss was found after temperature higher than 738 °C.

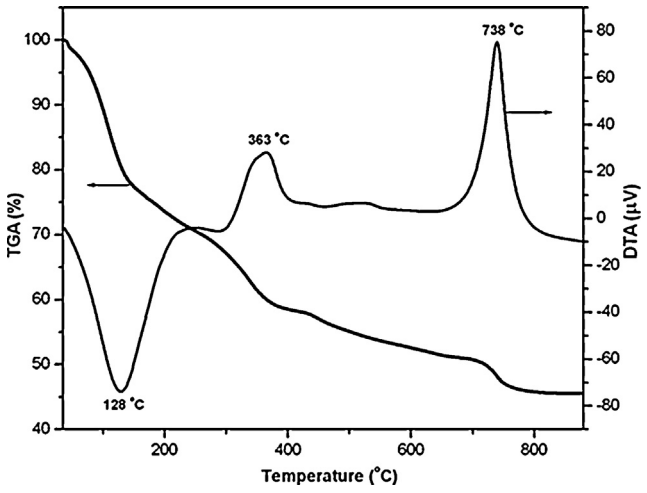

Fig. 3. Simultaneously recorded TGA/DTA cures of the carbonaceous precursor of $LaNbO_4$.

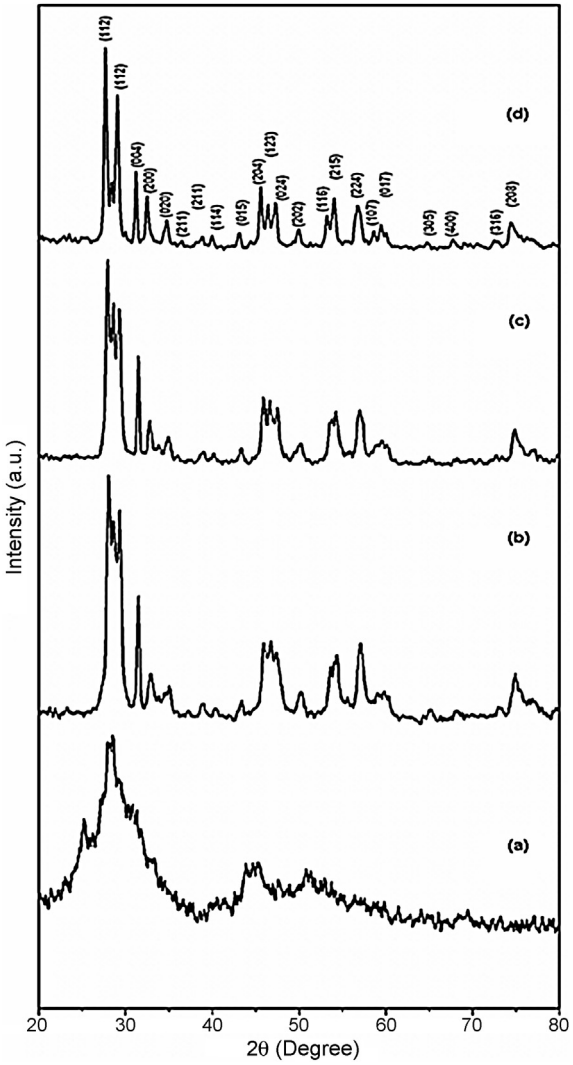

Fig. 4. X-ray diffraction patterns of $LaNbO_4$ precursor calcined at (a) 600 °C, (b) 700 °C, (c) 800 °C and (d) 900 °C.

Fig. 4 shows the XRD pattern of $LaNbO_4$ powder calcined at 600–900 °C for 2 h. The carbonaceous precursor of $LaNbO_4$, when calcined below 700 °C was amorphous. The diffraction patterns obtained after calcinations at 700 and 800 °C showed reflection peaks of both tetragonal and monoclinic phases of $LaNbO_4$ (JCPDS card No. 86-0911and 78-0158) [9]. It can be observed that the peaks at 2θ values of 29.05, 31.21, 34.74, 53.30 and 59.68 at 700 °C, and 29.05, 31.21, 40.04, 40.43, 46.46, 60.21 and 63.63 at 800 °C reflection show monoclinic phase crystallites. With increasing temperature the diffraction peaks of tetragonal gradually decrease whereas diffraction peaks of monoclinic become stronger. When the temperature reaches 900 °C monoclinic phase of $LaNbO_4$ is obtained, all the peaks were well consistent with standard JCPDS (card No. 78-0158) and no characteristic peak of impurities was observed. This confirmed the sample as pure monoclinic $LaNbO_4$ crystalline. This is considerably a lower temperature to obtain the monoclinic phase of $LaNbO_4$ compared with all previous report. The calculated lattice parameters [$a = 5.52$, $b = 5.15$ and $c = 11.47$] of the sample matched closely with the standard lattice parameter values. At higher calcination temperatures, XRD peaks became sharper without obvious extension in width. It can be concluded that the grain size and crystallinity increased with the calcination

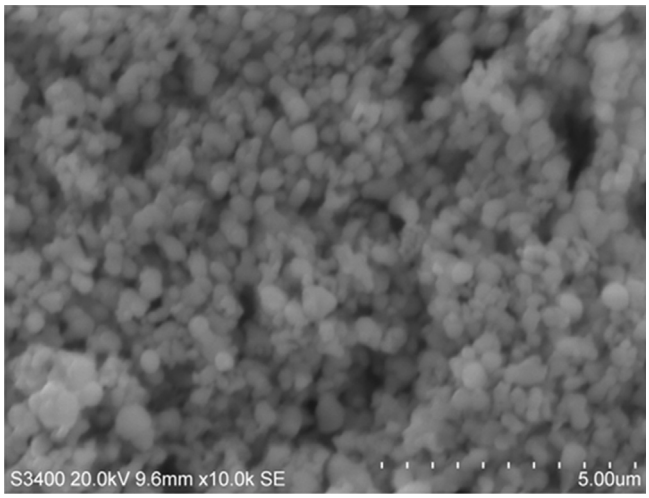

Fig. 5. SEM image of the $LaNbO_4$ nanopowder calcined at 900 °C.

temperature in the range of 700–900 °C. The crystalline size D, was determined by using the Scherrer equation;

$$D = \frac{0.9\lambda}{(B\cos\theta)} \quad (2)$$

where λ is the corrected wavelength of the X-ray radiation, B is the full width at half maximum corrected for instrumental broadening, and θ is the Bragg angle of the diffraction peak. The average sizes of the grain were calculated as 35, 42 and 62 nm for 700, 800 and 900 °C, respectively.

Fig. 5 shows a SEM micrograph of the calcined powder. The powder particles are found to be agglomerates of nano-sized primary particles. The particles were spherical-like structure with porous nature. TEM image of the prepared $LaNbO_4$ powder calcinated at 900 °C for 2 h is shown in Fig. 6. The image confirms the spherical shape of the particles, with uniform distribution. The average diameter of $LaNbO_4$ particles was found to be about 60 nm. The SAED pattern of the calcined sample is shown in Fig. 7. The diffraction pattern showed that the powder is well crystalline, and the observed plan confirmed the presence of crystal lattice of (1 1 2), (0 1 3) and (2 0 0) orientation. The observed diffraction plan revealed the monoclinic phase of the sample. This is consistent with the X-ray diffraction analysis.

The atomic % for La, Nb and O were found out from EDX (Fig. 8), and were 17.60, 17.50 and 64.90, respectively, ($La_{1.06}Nb_{1.05}O_{3.89}$), which was very close to the stoichiometric ratio of pure $LaNbO_4$.

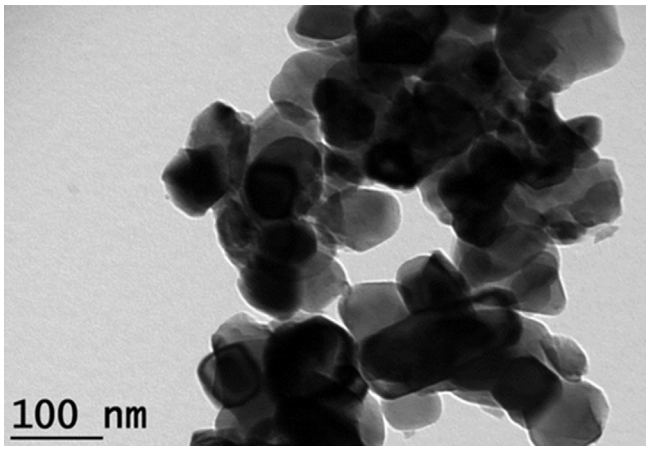

Fig. 6. TEM image of the $LaNbO_4$ nanopowder calcined at 900 °C.

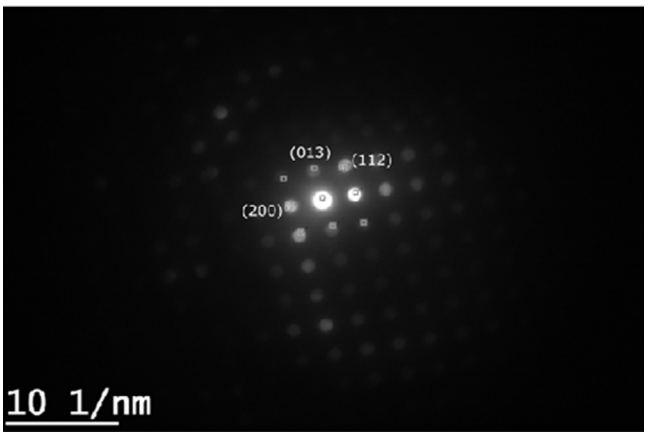

Fig. 7. SAED analysis of the $LaNbO_4$ nanopowder calcined at 900 °C.

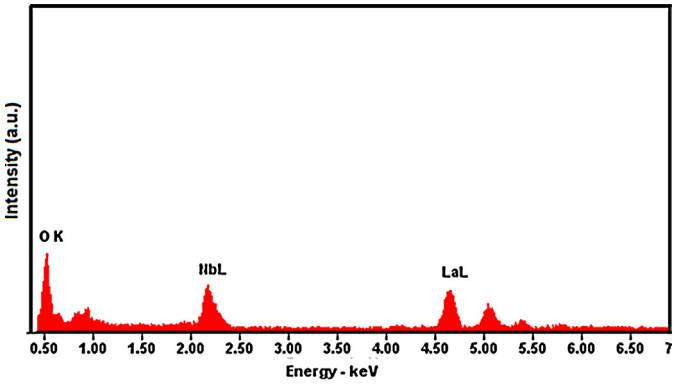

Fig. 8. EDX analysis of the $LaNbO_4$ nanopowder calcined at 900 °C.

The complex impedance plot of the $LaNbO_4$ nanopowder at 30 °C is shown in Fig. 9.The high frequency semi-circle absence indicates that the material conductivity depends on the grain boundaries. The resistance R of the sample was obtained from the intercept on the x-axis of the complex impedance plot. The conductivity of $LaNbO_4$ is calculated by using the following equation;

$$\sigma = \frac{L}{RA} \quad (3)$$

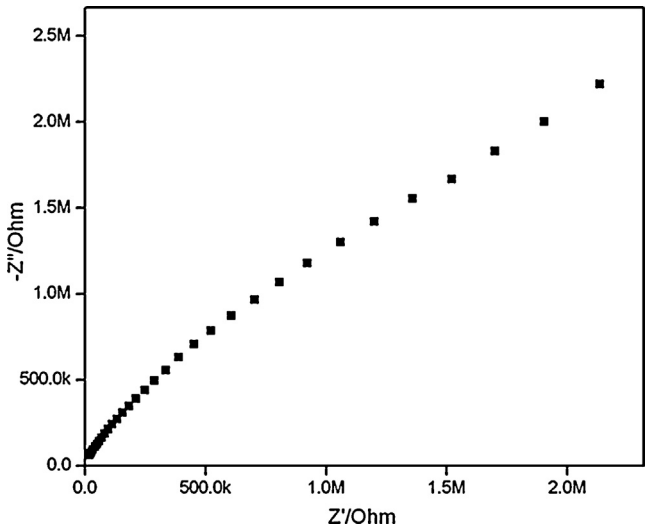

Fig. 9. Nyquist plot of the $LaNbO_4$ nanopowder obtained at 30 °C.

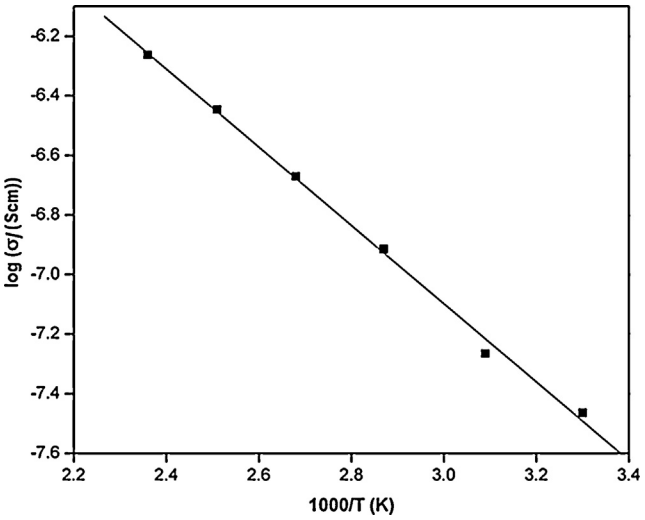

Fig. 10. Arrhenius plot of log conductivity versus reciprocal temperature for $LaNbO_4$.

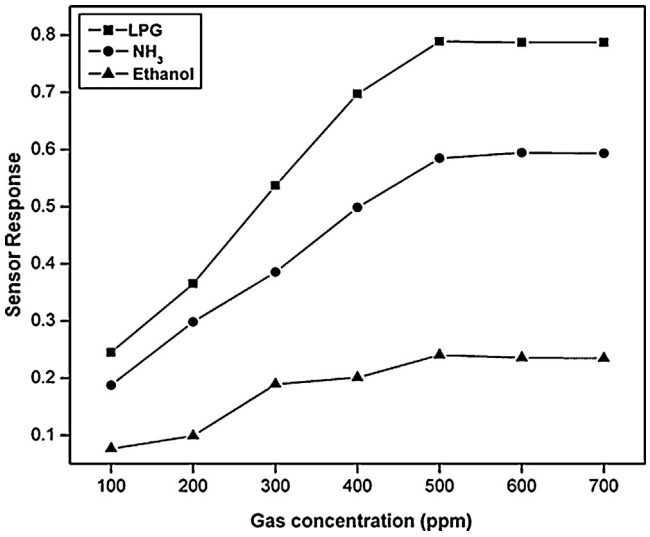

Fig. 12. Variation in gas response for LPG, NH_3 and ethanol gas as a function of gas concentrations at 250 °C.

where L and A are the thickness and known area of the sample. Electrical conductivity varied linearly as a function of temperature. It is noted from the Arrhenius plot that increased temperature increases the conductivity of the sample (Fig. 10). The activation energy of conduction process was calculated from the slope of $\log \sigma$ versus $1/T$ plot. In the temperature range of 30-175 °C, the activation energy of $LaNbO_4$ was found to be 0.29 eV. The observed temperature dependence on electrical conductivity is similar to those observed in semiconductor oxide systems. $LaNbO_4$ may behave as a semiconductor due to its oxygen deficiency [10]. The specific surface area of $LaNbO_4$ nanopowder calcined at 900 °C was estimated by Brunauer-Emmett-Teller (BET) method and it was found to be 24.36 m^2/g.

Fig. 11 shows the gas response versus operating temperature for $LaNbO_4$ based sensor for different test gases. At 250 °C, the highest gas sensitivity was observed for LPG (80%), followed by ammonia (59%) and ethanol (22%). This demonstrates that the response of $LaNbO_4$ based sensor to ammonia and ethanol at an operating temperature of 250 °C is very low compared to that of LPG. Fig. 12 shows the variation in gas response for LPG, NH_3 and ethanol gas as a function of gas concentrations at 250 °C. The sensitivity increased linearly with gas concentrations up to 500 ppm. The gas displayed the tendency to get saturated at concentrations above 500 ppm. The response of 500 ppm LPG was higher than that of 500 ppm NH_3 and ethanol, implying that the sensor was highly selective for LPG gas. The response and recovery times are important parameters in the design of sensors. The response is defined as the time taken to reach maximum response when the required amount of test gas is introduced into the chamber and keeping the sensor at operating temperature. The recovery time is the time taken by the sensor to come back to its initial value after the gas was removed. Fig. 13 depicts the response and recovery curves to 500 ppm LPG and NH_3 gas of $LaNbO_4$ sensor at an operating temperature 250 °C. When LPG gas was introduced, the response of the sensor increased and the maximum response time was less than 25 s. After the LPG gas was removed, the response gradually decreased and the recovery time to restore original value from the maximum response was less than 100 s. The response and recovery time for NH_3 was 10 s

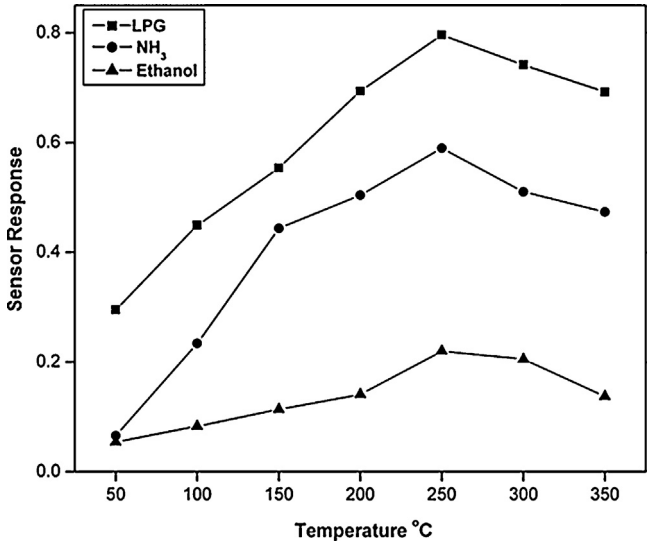

Fig. 11. Gas response characteristics of $LaNbO_4$ nanopowder for various reducing gases as a function of operating temperature.

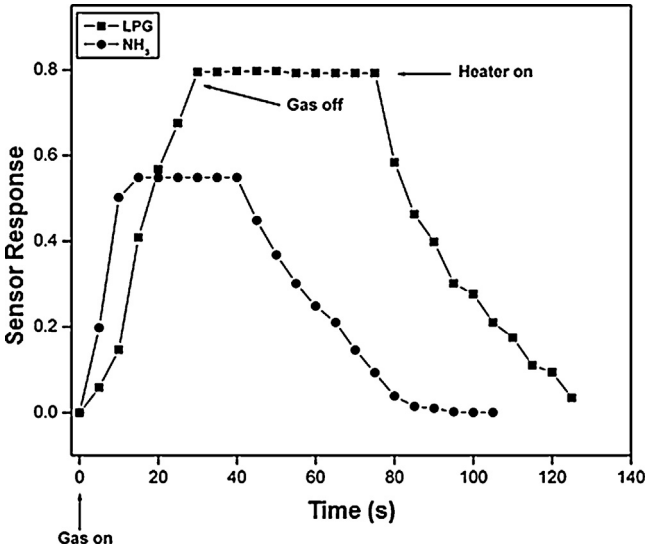

Fig. 13. Response and recovery of $LaNbO_4$ sensor as a function of time at their optimum operating temperatures for LPG and NH_3 gases.

and 80 s, respectively. It is well known that LPG consists of CH_4, C_3H_8, and C_4H_{10}, etc. and in these molecules the reducing hydrogen species are bound to carbon therefore LPG dissociates less easily into reactive reducing components on the $LaNbO_4$ Surface. Sensor materials are classified as n-type or p-type, depending on whether they show an increase or decrease in electrical resistance, when they are exposed to reducing test gases. In the present study, the $LaNbO_4$ nanopowder based sensor offered an increase in resistivity when test gases were introduced. Hence it behaved as a p-type sensor.

Metal oxide semiconductors are mainly used to detect small concentrations of reducing and combustible gases in air. In the absence of test gas, oxygen gets chemisorbed on the surface of oxide material and it extracts electrons from the conduction band, creating a depletion layer at the surface of the individual grains and the intergranular region. Thus, equilibrium of the chemisorptions process results in the stabilization of the surface resistance. The interactions between the test gas and sensing surface depend on the nature of physisorption, chemisorptions, surface defects and bulk defects. Physisorption is the weakest form of adsorption to sensor surface; no electrons are exchanged between the sensor material and the gas molecules. Hence, the conductivity of the sensor remains unchanged. Usually, physisorption monotonically decreases with increasing operating temperature. Chemisorption has a stronger interaction that shows a better sensitivity and selectivity. In chemisorptions, adsorbate forms chemical bonds with the surface atoms and thus the electronic structure of both the adsorbate and the surface are modified. Hence, defects on the surface play a more important role than bulk defects. The change in electrical conductivity of a material is given by;

$$\sigma = \sigma_o \exp\left(\frac{E_a}{kT}\right) P(O_2)^{1/n} \quad (4)$$

where σ is the electrical conductivity, E_a is the activation energy, k is Boltzmann's constant, T is the absolute temperature, $p_{(O_2)}$ is the partial pressure of O_2, and n depends on the nature of the point defects arising when O_2 is removed from the lattice.

When a sensor is exposed to air, oxygen molecules are adsorbed on the surface of the $LaNbO_4$. It traps electrons from the conduction band and produces negatively charged chemisorbed oxygen species such as O_2^-, O^- and O^{2-}, respectively. Hence, the concentration of holes in valence band increase and the resistance of the material decrease due to increased concentration of available carrier. The form of such chemisorbed oxygen species at the surface strongly depends on the operating temperature. At relatively lower operating temperature, the surface adsorbs more O_2^- and this causes the sensitivity to become low. As the temperature increases, both O^- and O^{2-} are chemisorbed. The adsorption of O^- was the most interesting process in sensors, because these oxygen ions were more reactive and thus made the material more sensitive to the presence of reducing gases. When $LaNbO_4$ is exposed to reducing gas, gas molecules react with adsorbed oxygen species on the surface and effective electron transfer occurs from the gas molecules to sensor material.

The surface reactions between the LPG and the oxygen species can be described as follows [11–13]:

$$C_nH_{2n+2} + 2O^- \rightarrow H_2O + C_nH_{2n}{:}\,O + e^- \quad (5)$$

$$C_nH_{2n}{:}\,O + O^- \rightarrow CO_2 + H_2O + e^- \quad (6)$$

Here, C_nH_{2n+2} represents CH_4, C_3H_8, C_4H_{10}, etc., while C_nH_{2n}:O represents partially oxidized intermediates on the $LaNbO_4$ surface.

The reaction between NH_3 and the chemisorbed oxygen O^- can take place as described below [14]:

$$2NH_3 + 3O^-_{(ads)} \rightarrow N_2 + 3H_2O + 3e^- \quad (7)$$

Electrons released from the above reaction are injected back into the conduction band of sensor material. These recombine with some of the holes, thus reducing the concentration of the charge carriers and decreasing the conduction of the sensor material, i.e., increasing electrical resistance of the p-type $LaNbO_4$ semiconductor. The maximum response for various gases depends on the availability of ionic species on the sensor surface which react with gas molecules. Compared to ammonia and ethanol, $LaNbO_4$ showed highest response for LPG at an operating temperature of 250 °C. This may be attributed to the availability of sufficient adsorbed ionic species of oxygen on the sensor surface which react most effectively with LPG molecules at this particular temperature. Beyond the optimum temperature, desorption of all oxygen ionic species occurs causing a decrease in response. The temperature plays an important role in the charge carrier concentration and the Debye length. This may be one of the reasons for the decrease in response of the $LaNbO_4$ sensor at higher temperature.

4. Conclusion

A novel nanocrystalline $LaNbO_4$ powder was prepared by using low temperature solution-based process. Typical monoclinic structure of $LaNbO_4$ was obtained at 900 °C for 2 h and it was confirmed by XRD and electron diffraction pattern of TEM analysis. The temperature dependent conductivity plots of the sample obeyed the Arrhenius relation. Sensitivity analysis showed that $LaNbO_4$ has a better response to LPG and NH_3 gases at an operating temperature of 250 °C than C_2H_5OH. The response times of LPG and NH_3 were about less than 25 and 10 s, respectively.

Novelty

Nanocrystalline $LaNbO_4$ prepared by low temperature process. Gas sensing behaviour of $LaNbO_4$ reported at the first time.

Acknowledgement

This work was supported by the WCU (World Class University) program, through a National Research Foundation of Korea (NRF) grant, funded by the Korea government (MEST) (No. R32-20087 and 2012R1A2A2A01014711).

References

[1] T. Mokkelbost, H.L. Lein, P.E. Vullum, R. Holmestad, T. Grande, M.-A. Einarsrud, Thermal and mechanical properties of $LaNbO_4$-based ceramics, Ceramics International 35 (2009) 2877–2883.
[2] Y.J. Hsiao, T.H. Fang, Y.S. Chang, Y.H. Chang, C.H. Liu, L.W. Ji, W.Y. Jywe, Structure and luminescent properties of $LaNbO_4$ synthesized by sol–gel process, Journal of Luminescence 126 (2007) 866–870.
[3] R. Haugsrud, T. Norby, Proton conduction in rare earth ortho-niobates and orthotantalates, Nature Materials 5 (2006) 193–196.
[4] R. Hauigsrud, T. Norby, High-temperature proton conductivity in acceptor-doped $LaNbO_4$, Solid State Ionics 177 (2006) 1129–1135.
[5] J.R. Tolchard, H. LeaLein, T. Grande, Chemical compatibility of proton conducting $LaNbO_4$ electrolyte with potential oxide cathodes, Journal of the European Ceramic Society 29 (2009) 2823–2830.
[6] T. Mokkelbost, Ø. Andersen, R.A. Strqm, K. Wiik, T. Grande, M. Einarsrud, High-temperature proton-conducting $LaNbO_4$-based materials: Powder synthesis by spray pyrolysis, Journal of American Ceramic Society 90 (2007) 3395–3400.
[7] R.N. Das, P. Pramanik, Chemical synthesis of fine powder of lead magnesium niobate using niobium tartarate complex, Materials Letters 46 (2000) 7–14.

[8] G.N. Chaudhari, S.V. Jagtap, N.N. Gedam, M.J. Pawar, V.S. Sangawar, Sol–gel synthesized semiconducting $LaCo_{0.8}Fe_{0.2}O_3$-based powder for thick film NH3 gas sensor, Talanta 78 (2009) 1136–1140.
[9] PCPDFWIN Version 2.4, JCPDS-ICDD (2003).
[10] V.V. Atuchin, I.E. Kalabin, V.G. Kesler, N.V. Pervukhina, Nb 3d and O 1s core levels and chemical bonding in niobates, Journal of Electron Spectroscopy and Related Phenomena 142 (2005) 129–134.
[11] P.P. Sahay, R.K. Nath, Al-doped zinc oxide thin films for liquid petroleum gas (LPG) sensors, Sensors and Actuators B: Chemical 133 (2008) 222–227.
[12] S.K. Biswas, P. Pramanik, Studies on the gas sensing behaviour of nanosized $CuNb_2O_6$ towards ammonia, hydrogen and liquefied petroleum gas, Sensors and Actuators B: Chemical 133 (2008) 449–455.
[13] M.R. Vaezi, S.K. Sadrnezhaad, Gas sensing behavior of nanostructured sensors based on tin oxide synthesized with different methods, Materials Science and Engineering B 140 (2007) 73–80.
[14] M.S. Wagh, G.H. Jain, D.R. Patil, L.A. Patil, Surface customization of SnO_2 thick films using RuO_2 as a surfactant for the LPG response, Sensors and Actuators B: Chemical 122 (2007) 357–364.